Published Online: 2025 October 15

Research Article

Astragaloside IV Improves Cyclophosphamide-Induced Liver Injury in Mice by Mediating Immunosuppression and Oxidative Stress Through the PI3K/Akt Signaling Pathway: A Randomized Trial

Yue e Sun [1], Jiahui Cao [1], Mengtao Li [1], Jingwen Ma [1], Weidong Wang [1,*]

[1] Xuzhou University of Technology, Jiangsu, China

[*] ***Corresponding Author:*** Xuzhou University of Technology, Jiangsu, China. Email: wangweidongwd@hotmail.com

Received: 26 July, 2025; **Revised:** 21 September, 2025; **Accepted:** 6 October, 2025

Abstract

Background: Cyclophosphamide (CTX) can lead to hepatotoxicity and low immunity. Astragaloside IV (AS-IV) can enhance the body's immune function.

Objectives: This study aimed to investigate whether AS-IV can improve CTX-induced liver injury in mice through the phosphoinositide 3-kinase (PI3K)/protein kinase B (Akt) signaling pathways and to explore whether its mechanism is related to immunosuppression and oxidative stress.

Methods: Forty-eight BALB/C mice aged 6 - 8 weeks were randomly divided into control groups, CTX group, AS-IV group, CTX+AS-IV low, medium, and high dose treatment groups, CTX+LY294002 group, and CTX+AS-IV-H+LY294002 group (n = 6 mice in each group). Mice in the control group and CTX group were given 1% starch paste by gavage daily. Mice in the AS-IV group and CTX+AS-IV groups were intragastrically administered AS-IV every day. Mice in the LY294002 group were intraperitoneally injected with LY294002 every 2 days. After 14 days, CTX was intraperitoneally injected for 2 consecutive days to induce a mouse liver injury model. The immune function of the mice was evaluated using HE staining and an Enzyme-Linked Immunosorbent Assay (ELISA) kit. The degree of oxidative stress and liver injury was detected by DHE fluorescent probe and ELISA kit. The PI3K/Akt axis protein expressions were detected using Western blot.

Results: Compared with the CTX group, AS-IV significantly increased the cytokines and immunoglobulin levels ($P < 0.05$) and reduced the levels of reactive oxygen species (ROS). Malondialdehyde (MDA) levels reduced from 0.788 nmol/mg to 0.475 nmol/mg, and liver injury indices increased. Superoxide dismutase (SOD) levels increased from 5.393 U/mg to 9.867 U/mg, and catalase (CAT) levels increased from 4.617 U/mg to 8.248 U/mg, restoring the integrity and clarity of liver cell structure ($P < 0.05$). The AS-IV also significantly increased protein levels; p-PI3K increased from 0.526 to 0.880, and p-Akt increased from 0.263 to 0.720. After LY294002 was applied on the basis of AS-IV intervention, CTX-caused liver damage was aggravated again. The cytokines, immunoglobulin, SOD, and CAT levels were significantly decreased, and the levels of liver injury indicators were significantly increased ($P < 0.05$).

Conclusions: The AS-IV improved CTX-induced immunosuppression and oxidative damage in mice by activating the PI3K/Akt axis and played a hepatoprotective role.

Keywords: Astragaloside IV, Liver Injury, PI3K/Akt Pathway, Immunosuppression, Oxidative Stress, Cyclophosphamide

1. Background

Cyclophosphamide (CTX) is an immunosuppressant and anticancer drug used clinically. The liver is the major site of CTX metabolism and also the target organ of its toxic effects (1, 2), which greatly limits its clinical application and therapeutic efficacy (3). Cytochrome P450 is present in the liver of mice (4). In mammalian livers, CTX is metabolized by cytochrome P450 into acrolein and phosphamide mustard (5). These metabolites have strong electrophilic abilities, which can promote lipid peroxidation in hepatocytes and bind

How to Cite: Sun Y E, Cao J, Li M, Ma J, Wang W. Astragaloside IV Improves Cyclophosphamide-Induced Liver Injury in Mice by Mediating Immunosuppression and Oxidative Stress Through the PI3K/Akt Signaling Pathway: A Randomized Trial. Hepat Mon. 2025; 25 (1): e164840. https://doi.org/10.5812/hepatmon-164840.

to the antioxidant glutathione (GSH) in exhausted liver tissue, resulting in small focal necrosis of hepatocytes and inflammatory cell infiltration (6). The CTX can also cause the liver to produce many reactive oxygen species (ROS), disrupt oxidative balance, induce oxidative stress in the liver, and cause drug-induced liver injury (7). Analysis revealed that CTX-induced liver injury is associated with oxidative stress imbalance. The immune system is an important protective mechanism of the human body. When immune function is impaired, immunosuppression occurs, which is manifested as persistent or transient immune dysfunction. The CTX kills small lymphocytes (LYMs) while targeting tumor cells. Due to its cytotoxic effects, its application often leads to abnormalities in blood routine, cytokines, and other indicators, resulting in a decline in the body's immune function. Immunosuppression is an important precipitating factor in the development of many diseases. Therefore, it is important to find drugs that can reduce CTX-induced liver injury and immunosuppression.

Astragaloside IV (AS-IV) is a natural saponin extracted from *Astragalus membranaceus*, which is the most active component of *A. membranaceus*. Clinically, it has been found that *A. membranaceus* improves liver function, enhances liver blood circulation, and delays liver fibrosis. At the same time, AS-IV is also the principal effective ingredient in Shenqi Fuzheng injection (SFI), which is commonly used in the clinical treatment of tumors. The SFI can activate tumor-infiltrating T LYMs to improve immunosuppression. Studies have shown that AS-IV has definite curative effects, including anti-oxidation and immune regulation (8-11). Previous studies have confirmed that AS-IV enhances immunity, activates the attack of immune cells on tumor cells, and reduces the resistance of tumors to chemotherapeutic drugs (12, 13). Moreover, AS-IV can alleviate cisplatin-induced renal injury, oxidative stress, and inflammation (14). The AS-IV can also play a hepatoprotective role by inhibiting oxidative stress and inflammation (15). Studies have confirmed that AS-IV can effectively inhibit ferroptosis and alleviate cisplatin-induced liver injury, inflammation, and oxidative stress (16). Furthermore, AS-IV can alleviate acute liver injury by regulating macrophage polarization and pyroptosis (17). The above experiments indicate that AS-IV may be a promising therapeutic option for liver injury and immunosuppression. However, the specific therapeutic effects and mechanisms of AS-IV on CTX-induced liver injury and immunosuppression are still unclear.

The phosphoinositide 3-kinase (PI3K)/protein kinase B (Akt) signaling pathway is involved in various pathological and physiological processes of liver injury and is a key target in the regulation of liver injury. The PI3K facilitates the synthesis of phosphatidylinositol-3,4,5-triphosphate (PIP3) at the cellular membrane. The phosphorylation of serine and threonine amino acids triggers the activation of Akt, assisted by a kinase that depends on PI3K. The Akt is activated by p-PI3K and transmits biological signals downstream, activating or inhibiting downstream signaling pathways. The PI3K exists in the cytoplasm and can activate T LYMs to produce a series of biological effects, such as promoting the proliferation of T LYMs, enhancing the antiviral ability of T LYMs, and activating its downstream molecule Akt. Studies have shown that activation of the PI3K/Akt pathway can significantly reverse sepsis-induced immunosuppression (18). Vitexin-2-O-rhamnoside can up-regulate the phosphorylation level of the PI3K/Akt signaling pathway and improve CTX-induced immunosuppression and oxidative stress (19). This indicates that the PI3K/Akt pathway is closely related to immune function. It was found that 25-Hydroxycholesterol 3-Sulfate could reduce the oxidation level and promote the recovery of liver function via the PI3K/Akt axis (20). Activation of the PI3K/Akt pathway can also improve liver injury by regulating inflammatory response, apoptosis, and oxidative stress (21-24). The above experiments demonstrate that the PI3K/Akt+ pathway is one of the mechanisms to improve liver injury. Further, studies have found that AS-IV can improve atherosclerosis and ulcerative colitis by regulating the PI3K/Akt pathway (25, 26). However, whether AS-IV can improve liver injury through the PI3K/Akt pathway is unknown.

Accordingly, this study speculates that AS-IV exerts a hepatoprotective effect in mice. The acute liver injury model of mice was established by pre-intervention with AS-IV and then CTX. The preventive effect of AS-IV on acute liver injury was observed, and its possible mechanism was discussed from the perspective of anti-oxidative stress and immunosuppression, offering novel insights for the prevention and therapy of liver injury

and providing theoretical bases for AS-IV medical practice.

2. Objectives

The focus of this study was to investigate the effects of AS-IV on CTX-induced liver injury, immunosuppression, oxidative stress, and the PI3K/Akt signaling pathway in mice. This study provides a new perspective on the mechanism by which AS-IV reduces liver injury.

3. Methods

3.1. Construction and Grouping of Animal Models

Forty-eight SPF BALB/C mice, aged 7 weeks and weighing 20 - 24 g, were purchased from Sberfo Biotechnology Co., Ltd. (Beijing, China). The animals were raised in the laboratory, and cages were used to acclimate the animals to the feeding conditions. The room temperature was maintained at 25 °C , with humidity levels between 40 - 60%, and a 12-hour day and night cycle was implemented. During the feeding period, the animals had free access to food and water. The animal experiment protocol of this study was approved by the School of Food and Biological Engineering, Xuzhou University of Technology Ethics Committee. After 1 week of adaptive feeding with ordinary maintenance feed, the mice were randomly divided into the control group, CTX group, AS-IV (AS-IV-H, 0.5 mg/kg) group, AS-IV low-dose treatment (CTX+AS-IV-L) group, AS-IV medium-dose treatment (CTX+AS-IV-M) group, AS-IV high-dose treatment (CTX+AS-IV-H) group, LY294002 intervention (CTX+LY294002) group, and AS-IV high-dose treatment + LY294002 intervention (CTX+AS-IV-H+LY294002) group. There were 6 mice in each group. Mice in the control group and CTX group were intragastrically administered 1% starch paste every day, while the remaining mice were intragastrically administered 25, 50, and 100 mg/kg AS-IV (S3901, Selleck, Shanghai, China) every day for 14 consecutive days. Additionally, mice in the LY294002 group were intraperitoneally injected with 25 mg/kg LY294002 (S1105, Selleck) every 2 days from day 1 to day 14. Subsequently, the CTX group was intraperitoneally injected with 100 mg/kg CTX (22011925, Hengrui Pharmaceutical Co., Ltd., Jiangxi, China) on the 14th and 15th days to induce liver injury, and the remaining mice were intraperitoneally injected with an equal volume of normal saline.

3.2. Tissue Sampling

Twenty-four hours after the last treatment, the mice in each group were fasted without water and anesthetized by intraperitoneal injection of 1% pentobarbital sodium (50 mg/kg). The eyeballs were extracted, and blood (about 500 µL) was collected, with the supernatant obtained after centrifugation. The mice were euthanized, and the liver, spleen, and thymus were dissected on a sterile operating table, weighed, and the Organ Index (organ weight/body weight) was calculated. Parts of the spleen, thymus, and middle part of the left hepatic lobe (2 mm × 2 mm × 2 mm) of the mice in each group were cut and placed in tissue fixative (G1101, Servicebio, Wuhan, China) for fixation, ethanol dehydration, xylene infiltration, and paraffin embedding, using 5 µm thickness sections for HE staining. The remaining fresh tissue was stored in a refrigerator at -80°C for subsequent experiments.

3.3. Determination of Whole Blood Index

Two hundred microliters of blood were taken from the eyeball and added to the anticoagulant tube, and then the whole blood automatic analyzer was used (TEK5000P, Tekang Technology Co., Ltd., Jiangxi, China). The white blood cell (WBC), platelet (PLT), LYM, red blood cell (RBC), hemoglobin (HGB), and granulocytes (Gran) were measured.

3.4. HE Staining

The spleen, thymus, and liver tissue sections of each group were immersed in hematoxylin (H3136, Sigma) for 3 minutes, differentiated in 1% hydrochloric acid ethanol, blue-backed in 0.6% ammonia water, and washed with pure water. Eosin dye solution (E4009, Sigma) was added dropwise for about 3 minutes, gradient dehydrated in ethanol, cleaned with xylene for 10 minutes, and sealed with neutral gum. A microscope (NIKON ECLIPSE E100, Nikon, Tokyo, Japan) was used to examine swelling, congestion, inflammatory cell infiltration, and vacuolization. The histopathological changes observed were evaluated using a semi-quantitative scoring system: No points, no liver cell damage; 1 point, < 10% of the regional cells showed vacuolization, swelling, congestion, and inflammatory

cell infiltration; 2 points, < 30% of the regional cells appeared vacuolization, swelling, congestion, inflammatory cell infiltration; 3 points, < 60% of the regional cells appeared vacuolization, swelling, congestion, inflammatory cell infiltration; 4 points, > 60% of the regional cells showed vacuolation, swelling, congestion, and inflammatory cell infiltration (27). The average was taken as the final score.

3.5. Spleen Cell Proliferation Assay

The spleen tissue of mice was taken on the ultra-clean bench, and the surrounding fat and connective tissue were removed. After thorough grinding, the LYM suspension was prepared using a 200-mesh sieve. The obtained spleen LYMs were diluted with an RPMI-1640 complete medium into a 3×10^6/mL cell suspension. One hundred microliters of cell suspension were inoculated into 96-well plates, 100 µL RPMI-1640 of complete culture medium was added to the control well, 80 µL RPMI-1640 of complete culture medium was added to the stimulation well, and 20 µL LPS (20 µg/mL) and ConA (50 µg/mL) were added to the stimulation well. Three replicates were set in each group. After incubation at 37°C for 20 hours, the LYM proliferation rate of mice was measured by an MTT cell detection kit. ConA-induced spleen cell proliferation reflects T LYM function, and LPS-induced spleen cell proliferation reflects B LYM function.

3.6. Enzyme-Linked Immunosorbent Assay

Interferon-γ (IFN-γ, ab282874, Abcam), interleukin (IL)-2 (ab100706, Abcam), IL-6 (ab222503, Abcam), IL-4 (ab100710, Abcam), IL-10 (ab255729, Abcam), IL-12 (ab100699, Abcam), immunoglobulin G (IgG, ab151276, Abcam), IgA (ab314603, Abcam), and IgM (ab133047, Abcam) Enzyme-Linked Immunosorbent Assay (ELISA) kits were employed to determine serum cytokine and immunoglobulin levels in mice. The standard used the same initial concentration and the same diluent, with a fixed dilution multiple to obtain the standard working solution. The sandwich ELISA technique was used in the kit: The capture antibody was coated on the microtiter plate to capture the analytes in the sample and the standard. After incubation and washing, the biotin-labeled detection antibody was added for incubation and washing to form the 'capture antibody-antigen-detection antibody' immune complex. Then, the streptavidin-coupled horseradish peroxidase was added for incubation. After the incubation was completed, the TMB chromogenic solution was added. If the analyte in the sample was present, it turned blue, and the termination solution was added to stop the reaction. The free components were washed away during the detection process, and the OD value was measured at 450 nm with a microplate reader. The color depth was proportional to the content of the analyte in the sample, and the concentration of the analyte in the sample was calculated by drawing a standard curve.

3.7. Kit Analysis

The mouse liver was homogenized with 0.9% sodium chloride solution, and the supernatant was collected after centrifugation. Simultaneously, the blood was centrifuged, and the supernatant was gathered in accordance with the instructions of content detection kits: 8-hydroxy-2'-deoxyguanosine (8-Oxo-dG, SEKSM-0038, Solarbio), malondialdehyde (MDA, BC0025, Solarbio), superoxide dismutase (SOD, BC5165, Solarbio), glutathione peroxidase (GSH-Px, BC1195, Solarbio), lactate dehydrogenase (LDH, BC0685, Solarbio), and aspartate aminotransferase (AST), alanine aminotransferase (ALT), alkaline phosphatase (ALP), nitric oxide (NO), and catalase (CAT; C010-2-1, C009-2-1, A059-2-2, A013-2-1, A007-1-1, Institute of Bioengineering, Nanjing, China). The oxidative stress and liver injury indices in the mouse livers were detected using a microplate reader (ELX808, BioTek, Beijing, China).

3.8. Dihydroethidium Fluorescent Staining

The level of ROS in the liver was measured using a superoxide anion probe DHE. The liver tissue was made into 5 µm frozen sections, washed with PBS buffer, and then treated with a 1:1000 DHE (S0063, Beyotime, Shanghai, China) working solution, incubated for 1 hour, and finally stained with DAPI. The expression of superoxide anion was observed under a fluorescence microscope, and ROS levels were analyzed using Image J software.

3.9. Western Blot

Liver and spleen tissues, each weighing 100 mg, were taken from mice and placed in a 5 mL sterile EP tube. A mixture of 100 µL of RIPA lysate (G20002, Servicebio), 1 µL of broad-spectrum enzyme inhibitor, and 1 µL of

phosphatase inhibitor was added in proportion and then lysed for 1 hour. Protein concentrations were measured using a BCA kit (G2026, Servicebio). Samples were diluted with a 5-fold loading buffer, boiled, denatured, separated by SDS-PAGE gel electrophoresis, transferred to a PVDF membrane, and blocked with 5% skim milk powder for 1 hour. Primary antibodies, including inducible nitric oxide synthase (iNOS, ab178945, Abcam), cyclooxygenase-2 (COX-2, ab283574, Abcam), PI3K (4292, Cell Signaling, Danvers, MA, USA), p-PI3K (4257, Cell Signaling), Akt (ab314110, Abcam), p-Akt (ab314038, Abcam), and GAPDH (ab9485, Abcam), were added. The membranes were incubated with an IgG-HRP-labeled protein secondary antibody (ab6734, Abcam) for 2 hours. The target protein bands were obtained by enhanced chemiluminescence (ECL, A38556, Thermo Fisher Scientific, Massachusetts, USA). ImageJ software was used to calculate the protein relative expressions.

3.10. Statistical Analysis

GraphPad Prism 9.0 statistical software was used for data analysis. Measurement data with normal distribution were expressed as mean ± standard deviation. One-way ANOVA analysis and Tukey tests were used for comparison among multiple groups. $P < 0.05$ was regarded as statistically significant.

4. Results

4.1. Astragaloside IV Ameliorated Cyclophosphamide-Induced Immunosuppression in Mice

After CTX induction, the counts of RBC, WBC, HGB, PLT, LYM, and Gran in the mouse blood were significantly decreased, as measured by an automatic analyzer, indicating that the immune response of the mice was weakened. After AS-IV treatment, the counts of RBC, WBC, HGB, PLT, LYM, and Gran were significantly increased and were close to the values of normal mice (Table 1).

The body weight, spleen, and Thymus indices of the mice markedly declined with CTX intervention. The AS-IV significantly increased the body weight, spleen, and Thymus Index of the mice in a dose-dependent manner (Figure 1A - C). In the CTX group, the spleen cell and thymocyte numbers of the mice decreased, necrotic areas without cell structure appeared, and the histological score increased significantly. In contrast, after AS-IV treatment, the spleen and thymus cells were arranged compactly and orderly, the nucleus was clear, and the intercellular space was small, comparable to normal mice (Figure 1D), and the histological score was significantly reduced (Appendices 1A and 1B in the Supplementary File). These results showed that AS-IV markedly attenuated CTX-induced spleen and thymus injury in mice, indicating that AS-IV enhanced immune function. After CTX intervention, the proliferation of spleen LYMs induced by ConA and LPS was significantly decreased, suggesting that CTX can reduce the function of T LYMs and B LYMs; after AS-IV treatment, there was a significant increase in T LYMs and B LYMs (Figure 1E and F). The CTX significantly reduced IFN-γ, IL-2, IL-6, IL-4, IL-10, IL-12, IgG, IgA, and IgM levels, while AS-IV significantly increased the levels of these indicators (Figure 1G - O). In conclusion, AS-IV can enhance CTX-induced immunosuppression in mice.

4.2. Astragaloside IV Attenuated Cyclophosphamide-Induced Liver Oxidative Stress

The CTX significantly increased the fluorescence intensity of DHE in liver tissue, indicating that the ROS level was significantly elevated; AS-IV significantly reduced the ROS level (Figure 2A and B). In addition, after CTX induction, the contents of MDA, NO, and 8-Oxo-dG increased significantly, while SOD, CAT, and GSH-Px levels decreased significantly. With AS-IV treatment, these indicators were significantly reversed (Figure 2C - H), suggesting that AS-IV could inhibit CTX-induced liver oxidative damage in mice.

4.3. Astragaloside IV Improved Cyclophosphamide-Induced Liver Injury

After CTX induction, the Liver Index of the mice was significantly decreased (Figure 3A), and AST, ALT, ALP, and LDH levels were obviously raised (Figure 3B - E), suggesting that the mouse livers were damaged and that AS-IV could ameliorate CTX-induced liver injury. After CTX intervention, the liver cells of the mice were loosely arranged, some cells were swollen and congested, cytoplasmic vacuolization was evident, the inflammatory reaction of the cells was significantly aggravated, vacuoles formed between the hepatocytes, and the histological score was significantly increased. After AS-IV treatment, the mouse livers improved

Table 1. The Effect of Astragaloside IV on the Amount of Immune Cells in the Blood of Cyclophosphamide-induced Mice (N = 6) [a]

Parameters	Control	CTX	AS-IV-H	CTX+AS-IV-L	CTX+AS-IV-M	CTX+AS-IV-H
RBC ($\times 10^{12}$/L)	11.56 ± 1.18	8.39 ± 0.07 [b]	12.09 ± 0.05	8.72 ± 0.15 [c]	9.41 ± 0.48 [d]	10.87 ± 0.54 [d]
WBC ($\times 10^{9}$/L)	10.83 ± 0.78	7.68 ± 0.50 [b]	10.02 ± 0.31	7.84 ± 0.08 [c]	9.15 ± 1.19 [d]	10.11 ± 1.06 [d]
HGB (g/L)	137.83 ± 3.47	124.45 ± 4.26 [b]	144.33 ± 4.12	126.68 ± 4.08 [c]	131.37 ± 5.23 [d]	135.17 ± 2.14 [d]
PLT ($\times 10^{9}$/L)	827.16 ± 18.15	538.16 ± 13.74 [b]	798.28 ± 21.22	547.33 ± 7.66 [c]	608.69 ± 14.61 [d]	725.35 ± 10.29 [d]
LYM ($\times 10^{9}$/L)	8.43 ± 0.25	5.57 ± 0.43 [b]	8.39 ± 0.32	5.82 ± 0.30 [c]	6.11 ± 0.24 [d]	6.37 ± 0.24 [d]
Gran ($\times 10^{9}$/L)	7.25 ± 0.28	6.83 ± 0.09 [b]	7.20 ± 0.31	6.92 ± 0.11 [c]	7.07 ± 0.07 [d]	7.13 ± 0.05 [d]

Abbreviations: CTX, cyclophosphamide; AS-IV, astragaloside IV; RBC, red blood cell; WBC, white blood cell; HGB, hemoglobin; PLT, platelet; LYM, lymphocyte; Gran, granulocytes.

[a] Values are expressed as mean ± SD.

[b] $P < 0.01$ vs. control group.

[c] $P < 0.05$ vs. CTX group.

[d] $P < 0.01$ vs. CTX group.

overall; the liver cell structure was relatively complete and clear, the arrangement was relatively neat, and the cellular inflammatory response was reduced (Figure 3F), with the histological score significantly reduced (Appendix 1C in the Supplementary File). In addition, AST, ALT, ALP, and LDH contents in the AS-IV-H group were consistent with those in the control group (Figure 3B - E), the liver cells were closely arranged, and the morphology was normal (Figure 3F), indicating that AS-IV showed no hepatotoxicity. Finally, iNOS and COX-2 protein levels were significantly increased after CTX induction and significantly decreased after AS-IV treatment, showing a dose-dependent manner (Figure 3G and H). In summary, AS-IV can significantly reduce CTX-induced hepatotoxicity.

4.4. Astragaloside IV Alleviated Cyclophosphamide-Induced Immunosuppression by Up-Regulating the Phosphoinositide 3-Kinase/Protein Kinase B Pathway in Mice

The CTX significantly reduced p-PI3K and p-Akt expressions in the liver and spleen tissues of mice, while AS-IV significantly increased p-PI3K and p-Akt expressions (Figure 4A - C), indicating that AS-IV could activate the PI3K/Akt axis in mice.

Due to the most pronounced hepatoprotective effect of 100 mg/kg AS-IV, this concentration was selected for subsequent experiments (28). Compared with the CTX group, the levels of p-PI3K and p-Akt protein in spleen tissue increased significantly after AS-IV treatment but decreased significantly after LY294002 intervention; compared with the CTX+AS-IV-H group, the levels of p-PI3K and p-Akt protein in the CTX+AS-IV-H+LY294002 group were also significantly decreased (Figure 5A and B). In addition, IFN-γ, IL-2, IL-4, IL-10, IL-12, IgG, and IgA levels in the CTX+AS-IV-H+LY294002 group were also significantly decreased (Figure 5C - I), indicating that suppression of the PI3K/Akt axis could weaken the AS-IV effect on CTX-induced immunosuppression. Thus, AS-IV can improve CTX-induced immunosuppression by activating the PI3K/Akt axis.

4.5. Astragaloside IV Improved Cyclophosphamide-Induced Oxidative Stress and Liver Injury by Up-Regulating the Phosphoinositide 3-Kinase/Protein Kinase B Pathway

Compared with CTX intervention, the p-PI3K and p-Akt proteins of the liver tissue were obviously decreased after LY294002 intervention. Compared with the CTX+AS-IV-H group, p-PI3K and p-Akt protein expressions of the CTX+AS-IV-H+LY294002 group were also significantly decreased (Figure 6A and B). After LY294002 treatment, the liver cells of the mice were loosely arranged again, and inflammatory cell infiltration, cell swelling, congestion, and vacuolization reoccurred. The pathological changes (Figure 6C) and histological scores (Appendix 1D in the Supplementary File) of the CTX+AS-IV-H+LY294002 group were between the CTX group and the CTX+AS-IV-H group. Compared with the CTX+AS-IV-H group, LY294002 significantly increased AST, ALT, ALP, and MDA contents, and significantly reduced SOD, CAT, and GSH-Px contents (Figure 6D - J). In summary, AS-IV can inhibit CTX-induced oxidative damage by activating the PI3K/Akt axis, thereby exerting hepatoprotective effects.

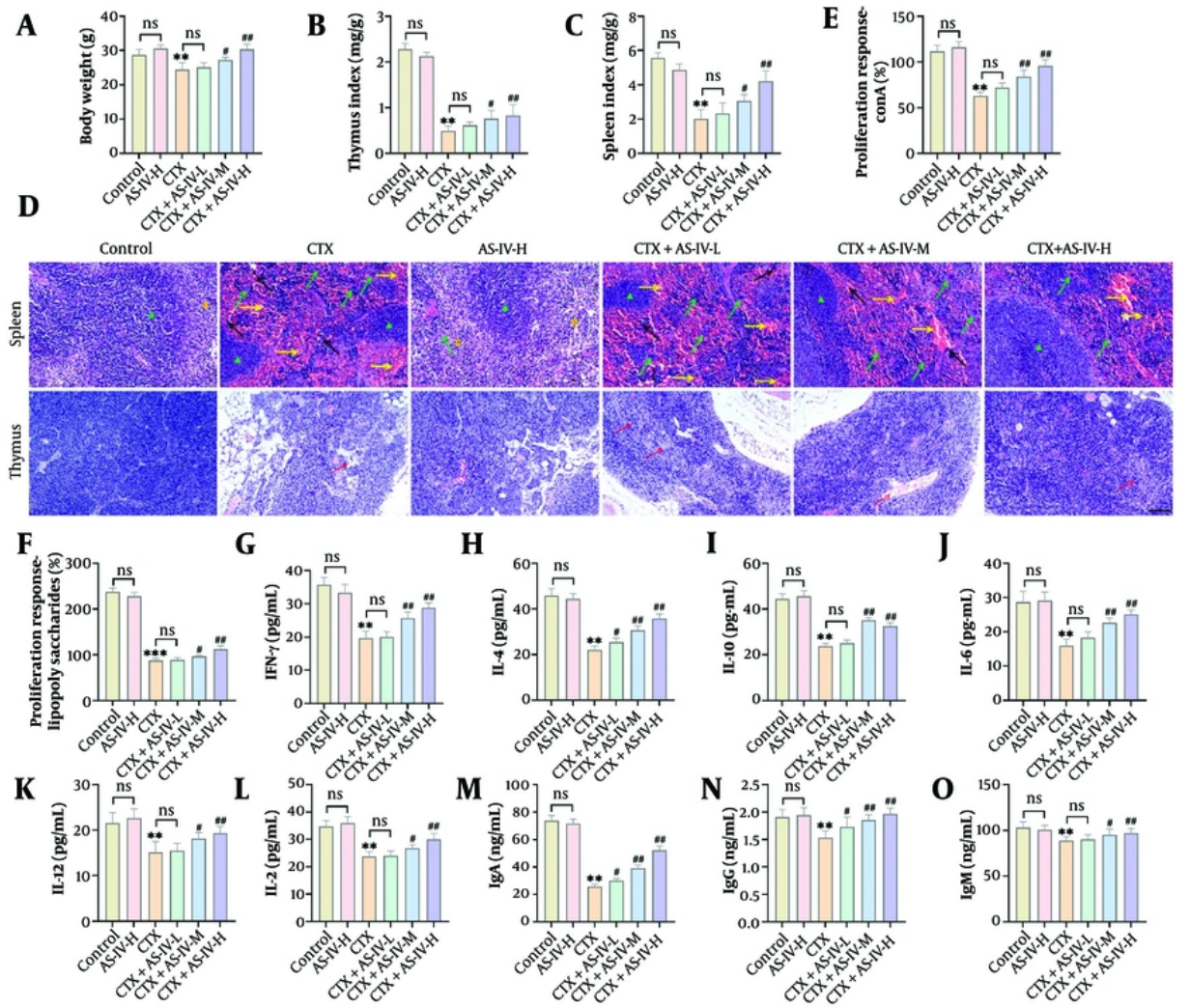

Figure 1. Astragaloside IV (AS-IV) ameliorated cyclophosphamide (CTX)-induced immunosuppression in mice: A - C, the final body weight of mice in each group was measured, and the spleen and thymus indices were calculated. The body weight, spleen, and Thymus Index of mice were significantly decreased after intraperitoneal injection of CTX and significantly increased after AS-IV treatment; D, the histological changes of the spleen and thymus were observed by HE staining. After CTX intervention, spleen cells and thymus cells decreased, and necrosis occurred. After AS-IV treatment, the spleen and thymus cells were arranged compactly, the nucleus was clear, and the intercellular space was small (× 20, 100 μm, green ▲: Red pulp; yellow #: White pulp; yellow →: Congestion; black →: Inflammatory infiltration; red →: Reduced cell density); E and F, the proliferation of spleen lymphocytes (LYMs) was detected by an Enzyme-Linked Immunosorbent Assay (ELISA) kit. T and B LYM proliferation decreased markedly after CTX induction and increased significantly after AS-IV treatment; G - O, the cytokines and immunoglobulins were detected by an ELISA kit. The contents of IFN-γ, IL-2, IL-6, IL-4, IL-10, IL-12, immunoglobulin G (IgG), IgA, and IgM were notably decreased after CTX induction and significantly increased after AS-IV treatment (n = 6, ns $P > 0.05$; ** $P < 0.01$ vs. control group; # $P < 0.05$, ## $P < 0.01$ vs. CTX group).

5. Discussion

The CTX cytotoxins can disrupt the body's immune system and cause immunodeficiency (29). The WBC constitute a key part of the body's defense system, with phagocytic activity and immune function as their main protective mechanisms. Among these WBCs, LYM are specialized immune cells that perform precise cellular and humoral immune responses to specific antigens and can eliminate foreign bodies. The RBC are the most abundant cell type in the blood, rich in HGB, and responsible for carrying oxygen and carbon dioxide. In addition to this transport function, RBCs also have certain immune defense capabilities and participate in

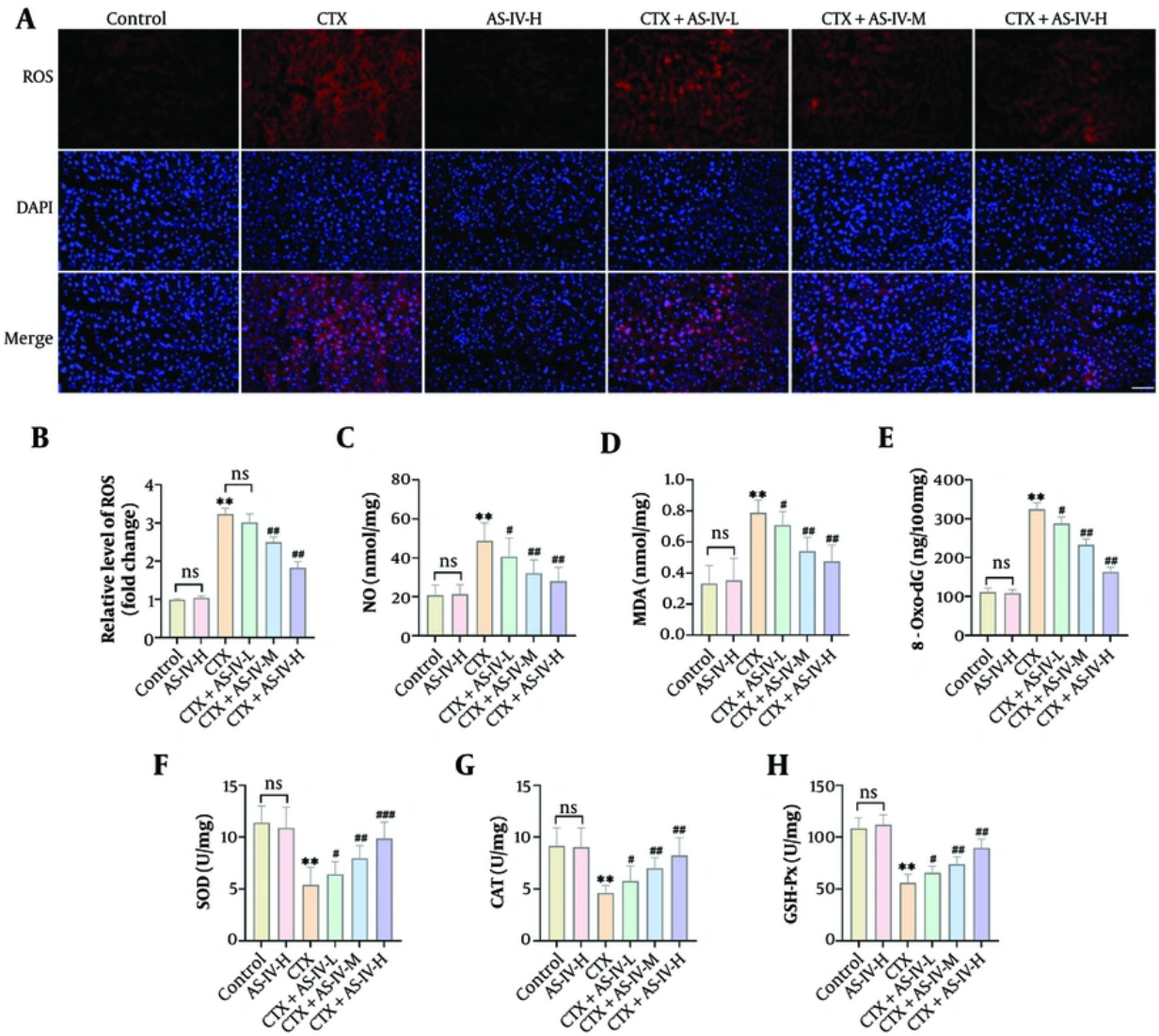

Figure 2. Astragaloside IV (AS-IV) attenuated cyclophosphamide (CTX)-induced liver oxidative stress: A and B, DHE fluorescent probe detected liver reactive oxygen species (ROS) levels, which increased significantly after CTX induction and decreased significantly after AS-IV treatment (× 40, 50 μm); C - H, the levels of oxidative damage indices in mouse liver tissue were measured using kits. It was observed that after CTX induction, the levels of malondialdehyde (MDA), nitric oxide (NO), and 8-hydroxy-2'-deoxyguanosine (8-Oxo-dG) increased significantly, while superoxide dismutase (SOD), catalase (CAT), and glutathione peroxidase (GSH-Px) levels decreased significantly. Following AS-IV treatment, Oxidative Damage Index levels were significantly reduced (n = 6, ns $P > 0.05$; ** $P < 0.01$ vs. control group; # $P < 0.05$, ## $P < 0.01$ vs. CTX group).

the immune processes of T and B cells. Therefore, they are essential elements of the immune system. The core function of PLT is to promote blood coagulation, form thrombi, and repair damaged blood vessels. The PLT surface can adsorb proteins and coagulation factor III required for coagulation, undergo activation deformation during vascular injury, increase surface viscosity, and form aggregates. Prothrombin is converted into thrombin by activating factor III on the surface, which further converts fibrinogen into fibrin and forms thrombi with other blood cells. It was found that CTX could significantly reduce the counts of WBC, RBC, and PLT in mice (30). The data from this research showed that RBC, WBC, HGB, PLT, LYM, and Gran counts

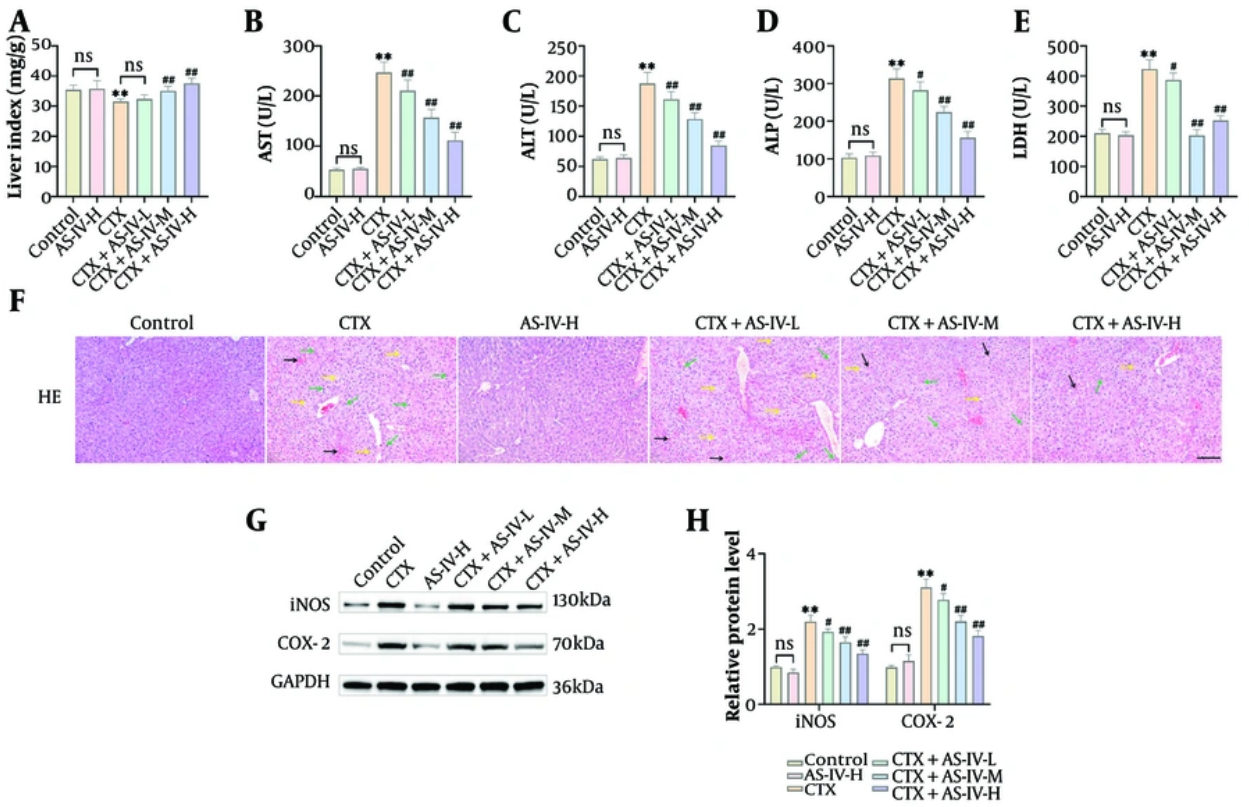

Figure 3. Astragaloside IV (AS-IV) improved cyclophosphamide (CTX)-induced liver injury: A, the Liver Index of mice was calculated. It decreased significantly after intraperitoneal injection of CTX and increased significantly after AS-IV treatment; B - E, the levels of liver injury indices were tested using kits. Aspartate aminotransferase (AST), alanine aminotransferase (ALT), alkaline phosphatase (ALP), and lactate dehydrogenase (LDH) levels were markedly elevated following CTX induction and decreased significantly after AS-IV treatment; F, the histological changes in the livers were observed using HE staining. Following CTX induction, liver cells were loosely arranged, with swelling, water ballooning, and inflammatory cell infiltration. The AS-IV could improve liver function (× 20, 100 μm, black →: Congestion; green →: Inflammatory cell infiltration; yellow →: Cell vacuolization, edema); G and H, Western blot (WB) detected inducible nitric oxide synthase (iNOS) and cyclooxygenase-2 (COX-2) protein levels in the liver, which showed that they increased significantly after CTX induction and decreased significantly after AS-IV treatment (n = 6, ns $P > 0.05$; ** $P < 0.01$ vs. control group; # $P < 0.05$, ## $P < 0.01$ vs. CTX group).

were significantly reduced, reflecting the inhibitory effect of CTX on immune function in rats. The AS-IV may have the effect of enhancing immunity.

Immunosuppression is accompanied by reduced body weight, impaired immune organs, reduced cytokine levels, and decreased LYM counts (31, 32). Liver injury is closely related to Body Mass Index (33). The thymus and spleen are two vital immune organs. Changes in their Organ Index reflect changes in macrophage proliferation rate and represent the strength of immune function. The spleen is the main site for the storage of T and B cells, while the thymus is where T LYMs mature. Additionally, spleen LYM proliferation is a vital stage in the immune response process. Therefore, the proliferation and differentiation of spleen LYMs can be used to evaluate immune function. ConA stimulates T LYM proliferation, and LPS stimulates B cell proliferation. The production of antibodies is a manifestation of humoral immunity. The determination of antibody levels can serve as an indicator of the body's humoral immunity level. The IgG and IgM antibodies in serum are the main antibodies produced in the first and second responses of the body, which are vital for the early and late stages of the immune response to infection. The levels of immunoglobulins such as IgG and IgA are important biomarkers for evaluating the state of the humoral immune response. Studies indicate that helper T cells are mainly classified into Th1 and Th2 subsets. Th1 mainly produces cytokines (IFN-γ, TNF-α, and IL-2) to

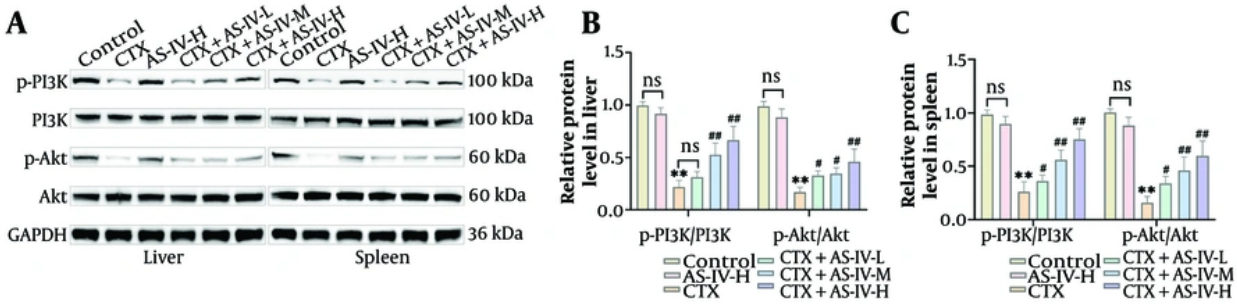

Figure 4. Astragaloside IV (AS-IV) activated phosphoinositide 3-kinase (PI3K)/protein kinase B (Akt) axis in mice: A - C, PI3K/Akt protein expressions in liver and spleen tissues were detected by WB. The p-PI3K and p-Akt levels were markedly decreased after cyclophosphamide (CTX) induction and significantly increased after AS-IV treatment (n = 6, ns $P > 0.05$; ** $P < 0.01$ vs. control group; # $P < 0.05$, ## $P < 0.01$ vs. CTX group).

assist cellular immunity, while Th2 mainly produces cytokines (IL-4, IL-5, IL-6, and IL-10) to assist humoral immunity (34, 35). IL-2, IL-6, and IL-12 stimulate the immune system, enhance immune cell activation and proliferation, and cause inflammatory responses (36). IFN-γ is a pro-inflammatory cytokine that promotes macrophage activation and regulates apoptosis and proliferation (37). The CTX can lead to immunosuppression in mice. The AS-IV can significantly ameliorate lymph injury, improve the condition of both the spleen and thymus in mice, enhance the humoral immune response, and reduce CTX-caused immunosuppression.

Oxidative stress is one of the mechanisms of liver injury, caused by excessive production of ROS. This persistent oxidative stress amplifies the inflammatory response (38). The SOD, CAT, and GSH-Px are important antioxidant defense enzymes (39). They can remove oxide molecules and maintain redox homeostasis. Therefore, they are widely used as markers for evaluating oxidative stress damage. Many studies have shown that oxidation is the key mechanism by which CTX exerts cytotoxicity and induces liver injury (40-42). The CTX stimulates the liver to produce many ROS and MDA. The former destroys the redox homeostasis of the liver, interferes with the antioxidant enzyme defense system with SOD and GSH-Px as the main members, and even leads to apoptosis. The latter destroys the cell membrane structure and further disrupts the balance of the antioxidant system. The 8-Oxo-dG is a biomarker of DNA oxidative injury and is widely used to assess oxidative stress levels (43). This research showed that AS-IV could significantly increase the activity of the liver antioxidant system and inhibit CTX-induced oxidative stress. Toxic chemicals can induce liver injury in rodents (44, 45). When inflammation, swelling, or necrosis occurs in hepatocytes, ALT and AST increase, indicating that the liver is injured (46, 47). The levels of ALP and LDH in serum can also reflect the degree of liver injury (48). Therefore, ALT, AST, ALP, and LDH are often used as key indicators to reflect liver function. Studies have shown that acute liver injury can be alleviated by regulating the expression of inflammatory factors (49, 50). Inhibition of iNOS and COX-2 activation can prevent the recruitment of inflammatory mediators in liver diseases, thereby improving liver function (51, 52). In this study, CTX increased hepatotoxicity, leading to impaired liver function. The AS-IV intervention could significantly increase the Liver Index of mice, reduce the pathological damage of hepatocytes, and reduce markers of liver injury.

This study also found that the PI3K/Akt axis contributed significantly to the hepatoprotective impact of AS-IV. The Akt is a key downstream signaling protein of PI3K (53). After activation, PI3K can bind to Akt in the plasma membrane. Activated Akt can lead to cytokine secretion imbalance and a series of inflammatory responses by regulating downstream factors and pathways (54). LY294002 is a broad-spectrum inhibitor of PI3K (55). The activation of many immune cells is affected by the PI3K/Akt pathway. Studies have shown that inhibition of the PI3K/Akt axis

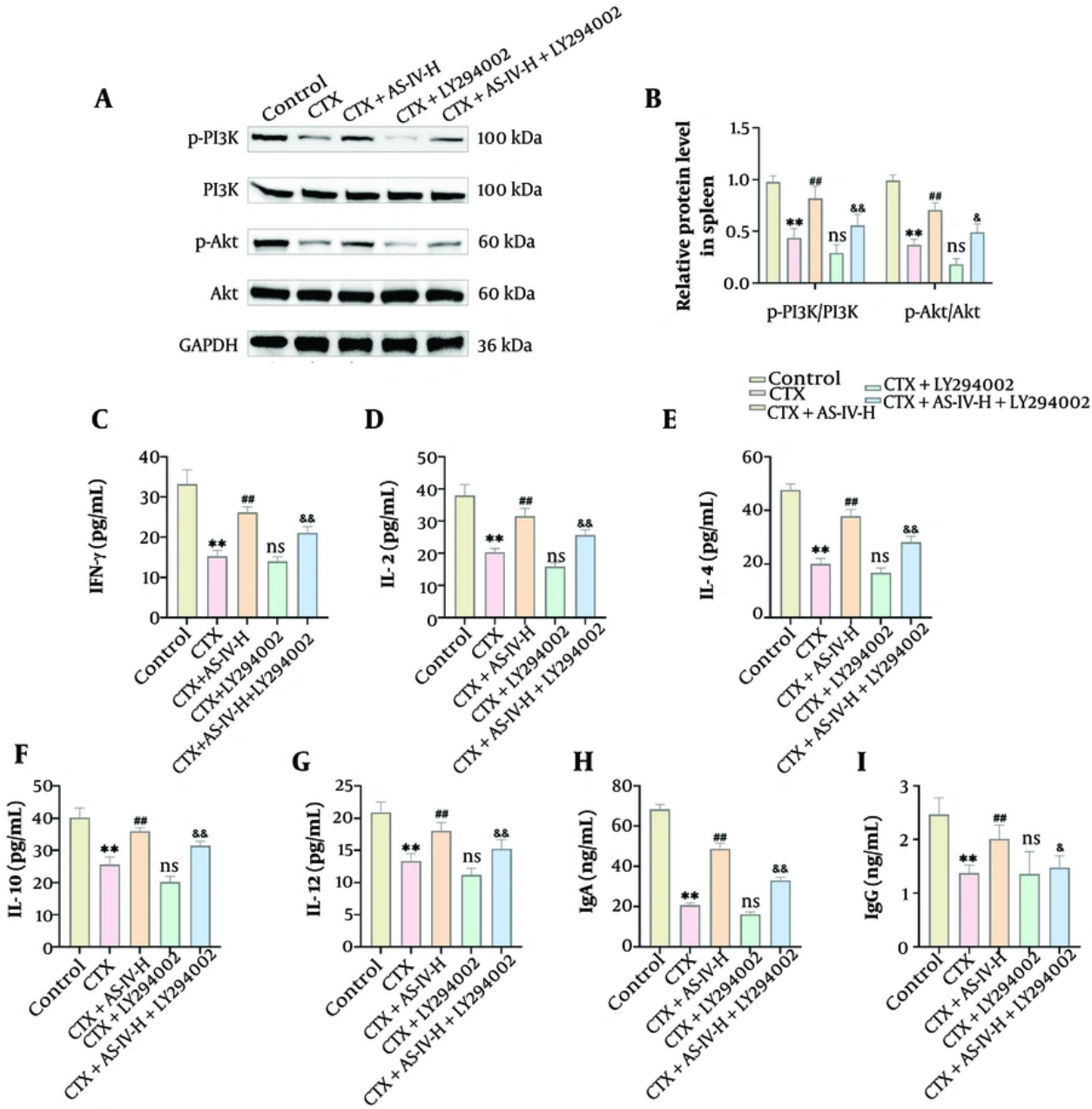

Figure 5. Astragaloside IV (AS-IV) alleviated cyclophosphamide (CTX)-induced immunosuppression by up-regulating the phosphoinositide 3-kinase (PI3K)/protein kinase B (Akt) pathway in mice: A and B, PI3K/Akt protein expressions in spleen tissue were detected by Western blot (WB). Compared with the CTX+AS-IV-H group, p-PI3K and p-Akt expressions significantly declined following LY294002 intervention; C - I, an Enzyme-Linked Immunosorbent Assay (ELISA) kit was used to detect cytokines and immunoglobulins. Compared with the CTX+AS-IV-H group, IFN-γ, IL-2, IL-4, IL-10, IL-12, immunoglobulin G (IgG), and IgA levels significantly decreased after LY294002 intervention (n = 6, ** $P < 0.01$ vs. control group; ns $P > 0.05$, # $P < 0.05$, ## $P < 0.01$ vs. CTX group; & $P < 0.05$, && $P < 0.01$ vs. CTX+AS-IV-H group).

inhibits LYM proliferation; promoting the PI3K/Akt pathway in the spleen can enhance immune function (19). The PI3K/Akt axis is also associated with the attenuation of liver injury. Leonurine can alleviate liver

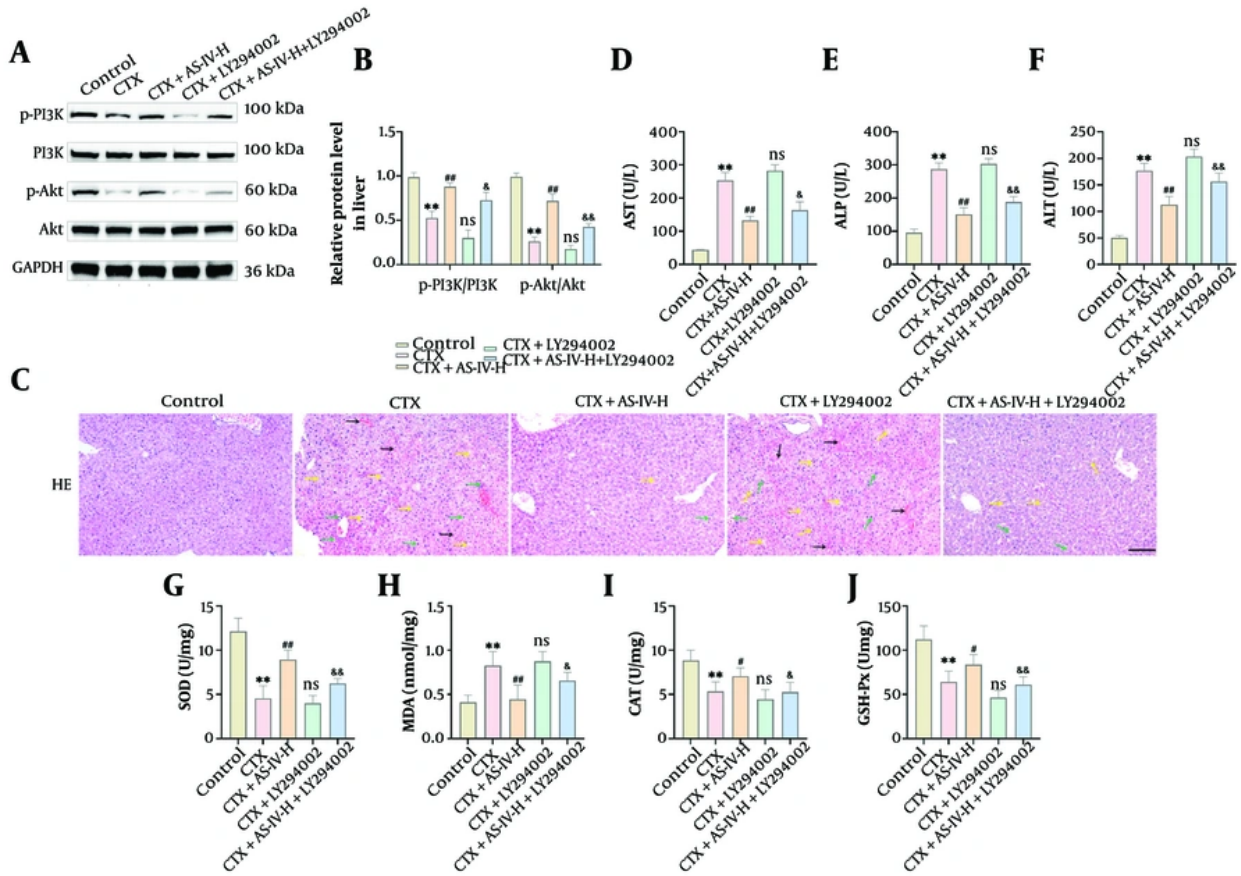

Figure 6. Astragaloside IV (AS-IV) improved cyclophosphamide (CTX)-induced oxidative stress and liver injury by up-regulating the phosphoinositide 3-kinase (PI3K)/protein kinase B (Akt) pathway: A and B, PI3K/Akt protein expressions in liver tissue were detected by WB. Data demonstrate that LY294002 can significantly reduce the levels of p-PI3K and p-Akt protein; C, the histological changes in mouse livers were observed by HE staining. After LY294002 intervention, liver tissue lesions were aggravated, inflammatory infiltration was raised, and cell arrangement was loose (× 20, 100 μm, black →: Congestion; green →: Inflammatory cell infiltration; yellow →: Cell vacuolization, edema); D - J, the liver injury indices and oxidative indices were measured using kits. Compared with the CTX+AS-IV-H group, LY294002 markedly raised aspartate aminotransferase (AST), alanine aminotransferase (ALT), alkaline phosphatase (ALP), and malondialdehyde (MDA) levels, and significantly decreased superoxide dismutase (SOD), catalase (CAT), and glutathione peroxidase (GSH-Px) levels (n = 6, ** $P < 0.01$ vs. control group; ns $P > 0.05$, # $P < 0.05$, ## $P < 0.01$ vs. CTX group; & $P < 0.05$, && $P < 0.01$ vs. CTX+AS-IV-H group).

injury, reverse hepatocyte necrosis, inflammatory response, and oxidative damage by triggering the PI3K/Akt pathway (21). *Ginkgo biloba* extract can also activate the PI3K/Akt pathway to alleviate inflammation and reduce liver injury (56). This study indicated that LY294002 significantly attenuated the enhanced immune response of AS-IV and mitigated oxidative stress and liver injury.

Moreover, the findings revealed that AS-IV can reduce CTX-induced liver injury. The AS-IV improves the body's cellular immunity and humoral immune function and enhances the immune response in mice. On the other hand, AS-IV can increase the activity of antioxidant enzymes and inhibit liver oxidative stress. Therefore, AS-IV may represent a potential adjunct treatment strategy, pending further mechanistic and clinical validation. However, this study has some limitations. The current conclusions are largely derived from mouse models. Due to the biological differences between humans and animals, drugs that work in animals may not necessarily work in humans. In the future, a humanized mouse model needs to be constructed to improve mechanistic research, and it is hoped that further clinical studies on AS-IV in the treatment of liver injury can be carried out to clarify its hepatoprotective effect in humans. At the

same time, it is necessary to monitor the cumulative effects and potential adverse reactions of AS-IV over an extended period and to explore the long-term effects of different concentrations of AS-IV.

5.1. Conclusions

To summarize, AS-IV significantly improved CTX-induced liver injury in mice by reducing oxidative injury and immunosuppression, with its mechanism correlated with the PI3K/Akt axis. This research offers new insights into the potential mechanism of AS-IV against CTX-induced liver injury, suggesting it as a candidate medication for drug-induced liver injury therapy. Although this study revealed the anti-liver injury mechanism of AS-IV to a certain extent, further studies using gene knockdown, transcriptome, and proteomics techniques are needed. The biochemical indicators and inhibition of PI3K/Akt signaling by LY294002 need to be further explained by compensation mechanisms or feedback loops.

Supplementary Material

Supplementary material(s) is available here [To read supplementary materials, please refer to the journal website and open PDF/HTML].

Footnotes

Authors' Contribution: Y. S. and J. C. edited and refined the manuscript with a focus on critical intellectual contributions. M. L. and J. M. participated in collecting, assessing, and interpreting the data and made significant contributions to data interpretation and manuscript preparation. J. C. and W. W. provided substantial intellectual input during the drafting and revision of the manuscript.

Conflict of Interests Statement: The authors declare no conflict of interest.

Data Availability: The data that support the findings of this study are available from the corresponding author upon reasonable request.

Ethical Approval: This study was approved by the School of Food and Biological Engineering, Xuzhou University of Technology Committee under the ethical approval code of KZ--2024032.

Funding/Support: This study was supported in part by grant KC22082 from the Key Research and Development Plan of Xuzhou city.

References

1. Zhai J, Song Z, Chang H, Wang Y, Han N, Liu Z, et al. He-Wei Granule enhances anti-tumor activity of cyclophosphamide by changing tumor microenvironment. *Chin Herb Med*. 2022;**14**(1):79-89. [PubMed ID: 36120121]. [PubMed Central ID: PMC9476702]. https://doi.org/10.1016/j.chmed.2021.10.002.
2. Zhang Y, Han Y, He J, Ouyang K, Zhao M, Cai L, et al. Digestive properties and effects of Chimonanthus nitens Oliv polysaccharides on antioxidant effects in vitro and in immunocompromised mice. *Int J Biol Macromol*. 2021;**185**:306-16. [PubMed ID: 34166692]. https://doi.org/10.1016/j.ijbiomac.2021.06.114.
3. Srirangan P, Sabina EP. Protective effects of herbal compounds against cyclophosphamide-induced organ toxicity: a pathway-centered approach. *Drug Chem Toxicol*. 2025;**48**(5):972-1014. [PubMed ID: 39847469]. https://doi.org/10.1080/01480545.2025.2455442.
4. Yi-Wen Z, Mei-Hua B, Xiao-Ya L, Yu C, Jing Y, Hong-Hao Z. Effects of Oridonin on Hepatic Cytochrome P450 Expression and Activities in PXR-Humanized Mice. *Biol Pharm Bull*. 2018;**41**(5):707-12. [PubMed ID: 29709908]. https://doi.org/10.1248/bpb.b17-00882.
5. Murray M, Butler AM, Stupans I. Competitive inhibition of human liver microsomal cytochrome P450 3A-dependent steroid 6 beta-hydroxylation activity by cyclophosphamide and ifosfamide in vitro. *J Pharmacol Exp Ther*. 1994;**270**(2):645-9. [PubMed ID: 8071856].
6. Senthilkumar S, Devaki T, Manohar BM, Babu MS. Effect of squalene on cyclophosphamide-induced toxicity. *Clin Chim Acta*. 2006;**364**(1-2):335-42. [PubMed ID: 16150433]. https://doi.org/10.1016/j.cca.2005.07.032.
7. Saleh AK, El-Mahdy NA, El-Masry TA, El-Kadem AH. Trifluoperazine mitigates cyclophosphamide-induced hepatic oxidative stress, inflammation, and apoptosis in mice by modulating the AKT/mTOR-driven autophagy and Nrf2/HO-1 signaling cascades. *Life Sci*. 2024;**344**:122566. [PubMed ID: 38499285]. https://doi.org/10.1016/j.lfs.2024.122566.
8. Zhang J, Wu C, Gao L, Du G, Qin X. Astragaloside IV derived from Astragalus membranaceus: A research review on the pharmacological effects. *Adv Pharmacol*. 2020;**87**:89-112. [PubMed ID: 32089240]. https://doi.org/10.1016/bs.apha.2019.08.002.
9. Granhoj JS, Witness Praest Jensen A, Presti M, Met O, Svane IM, Donia M. Tumor-infiltrating lymphocytes for adoptive cell therapy: recent advances, challenges, and future directions. *Expert Opin Biol Ther*. 2022;**22**(5):627-41. [PubMed ID: 35414331]. https://doi.org/10.1080/14712598.2022.2064711.
10. Meng P, Yang R, Jiang F, Guo J, Lu X, Yang T, et al. Molecular Mechanism of Astragaloside IV in Improving Endothelial Dysfunction of Cardiovascular Diseases Mediated by Oxidative Stress. *Oxid Med Cell Longev*. 2021;**2021**:1481236. [PubMed ID: 34840664]. [PubMed Central ID: PMC8626190]. https://doi.org/10.1155/2021/1481236.
11. Tan YQ, Chen HW, Li J. Astragaloside IV: An Effective Drug for the Treatment of Cardiovascular Diseases. *Drug Des Devel Ther*.

2020;**14**:3731-46. [PubMed ID: 32982178]. [PubMed Central ID: PMC7507407]. https://doi.org/10.2147/DDDT.S272355.

12. Xu F, Cui WQ, Wei Y, Cui J, Qiu J, Hu LL, et al. Correction: Astragaloside IV inhibits lung cancer progression and metastasis by modulating macrophage polarization through AMPK signaling. *J Exp Clin Cancer Res*. 2023;**42**(1):70. [PubMed ID: 36959638]. [PubMed Central ID: PMC10035129]. https://doi.org/10.1186/s13046-023-02643-y.
13. Liu F, Ran F, He H, Chen L. Astragaloside IV Exerts Anti-tumor Effect on Murine Colorectal Cancer by Re-educating Tumor-Associated Macrophage. *Arch Immunol Ther Exp*. 2020;**68**(6):33. [PubMed ID: 33095374]. https://doi.org/10.1007/s00005-020-00598-y.
14. Arda DB, Bora ES, Imaz G, Topal F, Erba O. Exploring the Protective Effects of Astragaloside IV against Cisplatin-Induced Kidney Injury in Rats. *Int J Pharmacol*. 2024;**20**(7):1331-8. https://doi.org/10.3923/ijp.2024.1331.1338.
15. Sun Y, Ma Y, Sun F, Feng W, Ye H, Tian T, et al. Astragaloside IV attenuates lipopolysaccharide induced liver injury by modulating Nrf2-mediated oxidative stress and NLRP3-mediated inflammation. *Heliyon*. 2023;**9**(4). e15436. [PubMed ID: 37113780]. [PubMed Central ID: PMC10126932]. https://doi.org/10.1016/j.heliyon.2023.e15436.
16. Guo J, Le Y, Yuan A, Liu J, Chen H, Qiu J, et al. Astragaloside IV ameliorates cisplatin-induced liver injury by modulating ferroptosis-dependent pathways. *J Ethnopharmacol*. 2024;**328**:118080. [PubMed ID: 38521426]. https://doi.org/10.1016/j.jep.2024.118080.
17. Kuang G, Zhao Y, Wang L, Wen T, Liu P, Ma B, et al. Astragaloside IV Alleviates Acute Hepatic Injury by Regulating Macrophage Polarization and Pyroptosis via Activation of the AMPK/SIRT1 Signaling Pathway. *Phytother Res*. 2025;**39**(2):733-46. [PubMed ID: 39660635]. https://doi.org/10.1002/ptr.8403.
18. Fu XZ, Wang Y. Interferon-gamma regulates immunosuppression in septic mice by promoting the Warburg effect through the PI3K/AKT/mTOR pathway. *Mol Med*. 2023;**29**(1):95. [PubMed ID: 37434129]. [PubMed Central ID: PMC10337057]. https://doi.org/10.1186/s10020-023-00690-x.
19. Wang Y, Ni W, Jin X, Li J, Yu Y. Vitexin-2-O-rhamnoside improves immunosuppression, oxidative stress, and phosphorylation of PI3K/Akt signal pathway in cyclophosphamide treated mice. *Eur J Pharmacol*. 2022;**925**:174999. [PubMed ID: 35525311]. https://doi.org/10.1016/j.ejphar.2022.174999.
20. Wang Y, Pandak WM, Lesnefsky EJ, Hylemon PB, Ren S. 25-Hydroxycholesterol 3-Sulfate Recovers Acetaminophen Induced Acute Liver Injury via Stabilizing Mitochondria in Mouse Models. *Cells*. 2021;**10**(11). [PubMed ID: 34831255]. [PubMed Central ID: PMC8616185]. https://doi.org/10.3390/cells10113027.
21. Yu Y, Zhou S, Wang Y, Di S, Wang Y, Huang X, et al. Leonurine alleviates acetaminophen-induced acute liver injury by regulating the PI3K/AKT signaling pathway in mice. *Int Immunopharmacol*. 2023;**120**:110375. [PubMed ID: 37267857]. https://doi.org/10.1016/j.intimp.2023.110375.
22. Song Y, Mao Y, Sui Q, Zhao Z, Dong D. ALA Alleviates Liver Damage in Septic Mice Through PI3K/AKT Signaling Pathway. *Food Sci Nutr*. 2025;**13**(7). e70599. [PubMed ID: 40654536]. [PubMed Central ID: PMC12245727]. https://doi.org/10.1002/fsn3.70599.
23. Zhang R, Sun X, Lu H, Zhang X, Zhang M, Ji X, et al. Akkermansia muciniphila Mediated the Preventive Effect of Disulfiram on Acute Liver Injury via PI3K/Akt Pathway. *Microb Biotechnol*. 2025;**18**(1). e70083. [PubMed ID: 39825784]. [PubMed Central ID: PMC11748400]. https://doi.org/10.1111/1751-7915.70083.
24. Yin Y, Mu F, Zhang L, Zhao J, Gong R, Yin Y, et al. Wedelolactone activates the PI3K/AKT/NRF2 and SLC7A11/GPX4 signalling pathways to alleviate oxidative stress and ferroptosis and improve sepsis-induced liver injury. *J Ethnopharmacol*. 2025;**344**:119557. [PubMed ID: 40010556]. https://doi.org/10.1016/j.jep.2025.119557.
25. Sun D, Wang Y, Pang B, Jiang L. Astragaloside IV Mediates the PI3K/Akt/mTOR Pathway to Alleviate Injury and Modulate the Composition of Intestinal Flora in ApoE(-/-) Atherosclerosis Model Rats. *Discov Med*. 2024;**36**(184):1070-9. [PubMed ID: 38798265]. https://doi.org/10.24976/Discov.Med.202436184.99.
26. Zhang X, Zhang F, Li Y, Fan N, Zhao K, Zhang A, et al. Blockade of PI3K/AKT signaling pathway by Astragaloside IV attenuates ulcerative colitis via improving the intestinal epithelial barrier. *J Transl Med*. 2024;**22**(1):406. [PubMed ID: 38689349]. [PubMed Central ID: PMC11061986]. https://doi.org/10.1186/s12967-024-05168-w.
27. He J, Huang Z, Zou R. Andrographolide ameliorates sepsis-induced acute liver injury by attenuating endoplasmic reticulum stress through the FKBP1A-mediated NOTCH1/AK2 pathway. *Cell Biol Toxicol*. 2025;**41**(1):56. [PubMed ID: 40053226]. [PubMed Central ID: PMC11889056]. https://doi.org/10.1007/s10565-025-10007-9.
28. Yao J, Liu J, He Y, Liu L, Xu Z, Lin X, et al. Systems pharmacology reveals the mechanism of Astragaloside IV in improving immune activity on cyclophosphamide-induced immunosuppressed mice. *J Ethnopharmacol*. 2023;**313**:116533. [PubMed ID: 37100262]. https://doi.org/10.1016/j.jep.2023.116533.
29. Li Y, Yu P, Fu W, Cai L, Yu Y, Feng Z, et al. Ginseng-Astragalus-oxymatrine injection ameliorates cyclophosphamide-induced immunosuppression in mice and enhances the immune activity of RAW264.7 cells. *J Ethnopharmacol*. 2021;**279**:114387. [PubMed ID: 34216728]. https://doi.org/10.1016/j.jep.2021.114387.
30. M R, S S, Jose SP, S S, Asish A, Jalam JK, et al. Immunomodulatory Effect of a Polyherbal Formulation (Imusil) on Cyclophosphamide Induced Experimental Animal Model. *Asian Pac J Cancer Prev*. 2023;**24**(11):3729-38. [PubMed ID: 38019230]. [PubMed Central ID: PMC10772766]. https://doi.org/10.31557/APJCP.2023.24.11.3729.
31. Ali MS, Lee EB, Quah Y, Sayem SAJ, Abbas MA, Suk K, et al. Modulating effects of heat-killed and live Limosilactobacillus reuteri PSC102 on the immune response and gut microbiota of cyclophosphamide-treated rats. *Vet Q*. 2024;**44**(1):1-18. [PubMed ID: 38682319]. [PubMed Central ID: PMC11060015]. https://doi.org/10.1080/01652176.2024.2344765.
32. Stepanenko AA, Sosnovtseva AO, Valikhov MP, Chernysheva AA, Abramova OV, Pavlov KA, et al. Systemic and local immunosuppression in glioblastoma and its prognostic significance. *Front Immunol*. 2024;**15**:1326753. [PubMed ID: 38481999]. [PubMed Central ID: PMC10932993]. https://doi.org/10.3389/fimmu.2024.1326753.
33. Jiang Y, Chen R, Xu S, Ding Y, Zhang M, Bao M, et al. Endocrine and metabolic factors and the risk of idiopathic pulmonary fibrosis: a Mendelian randomization study. *Front Endocrinol*. 2023;**14**:1321576. [PubMed ID: 38260151]. [PubMed Central ID: PMC10801027]. https://doi.org/10.3389/fendo.2023.1321576.
34. Dong Y, Tang Y, Li Y, Cao P, Xu G, Zhu R, et al. Role of peripheral cytokines and orbitofrontal cortex subregion structure in schizophrenia agitation. *Sci Rep*. 2025;**15**(1):14125. [PubMed ID:

40269239]. [PubMed Central ID: PMC12019167]. https://doi.org/10.1038/s41598-025-99033-5.

35. Teng F, Jin Q. Evaluation of cytokine expressions in patients with recurrent aphthous stomatitis: A systematic review and meta-analysis. *PLoS One*. 2024;**19**(6). e0305355. [PubMed ID: 38861558]. [PubMed Central ID: PMC11166324]. https://doi.org/10.1371/journal.pone.0305355.
36. Al-Qahtani AA, Alhamlan FS, Al-Qahtani AA. Pro-Inflammatory and Anti-Inflammatory Interleukins in Infectious Diseases: A Comprehensive Review. *Trop Med Infect Dis*. 2024;**9**(1). [PubMed ID: 38251210]. [PubMed Central ID: PMC10818686]. https://doi.org/10.3390/tropicalmed9010013.
37. Ng CT, Fong LY, Abdullah MNH. Interferon-gamma (IFN-gamma): Reviewing its mechanisms and signaling pathways on the regulation of endothelial barrier function. *Cytokine*. 2023;**166**:156208. [PubMed ID: 37088004]. https://doi.org/10.1016/j.cyto.2023.156208.
38. Wang J, Tao X, Liu Z, Yan Y, Cheng P, Liu B, et al. Noncoding RNAs in sepsis-associated acute liver injury: Roles, mechanisms, and therapeutic applications. *Pharmacol Res*. 2025;**212**:107596. [PubMed ID: 39800175]. https://doi.org/10.1016/j.phrs.2025.107596.
39. Tang Y, Zhao R, Pu Q, Jiang S, Yu F, Yang Z, et al. Investigation of nephrotoxicity on mice exposed to polystyrene nanoplastics and the potential amelioration effects of DHA-enriched phosphatidylserine. *Sci Total Environ*. 2023;**892**:164808. [PubMed ID: 37308008]. https://doi.org/10.1016/j.scitotenv.2023.164808.
40. Huang Y, Ma C, Zhu L, Kong L, Huang C, Yang W, et al. The Ameliorative Effect of Betulinic Acid on Oxidative Stress in Mice of Cyclophosphamide-Induced Liver Damage. *Environ Toxicol*. 2025;**40**(4):608-23. [PubMed ID: 39601349]. https://doi.org/10.1002/tox.24444.
41. Alshehri MA, Alissa M, Alghamdi A. Resveratrol attenuates cyclophosphamide-induced hepatic apoptosis in association with the inhibition of oxidative stress and inflammation in a rat model of acute liver injury. *Tissue Cell*. 2025;**93**:102728. [PubMed ID: 39808867]. https://doi.org/10.1016/j.tice.2025.102728.
42. Cheng M, Zheng Y, Wu G, Tan L, Xu F, Zhang Y, et al. Protective Effect of Artocarpus heterophyllus Lam. (Jackfruit) Polysaccharides on Liver Injury Induced by Cyclophosphamide in Mice. *Nutrients*. 2024;**16**(1). [PubMed ID: 38201995]. [PubMed Central ID: PMC10780714]. https://doi.org/10.3390/nu16010166.
43. Yadav V, Krishnan A, Zahiruddin S, Ahmad S, Vohora D. Amelioration of cyclophosphamide-induced DNA damage, oxidative stress, and hepato- and neurotoxicity by Piper longum extract in rats: The role of gammaH2AX and 8-OHdG. *Front Pharmacol*. 2023;**14**:1147823. [PubMed ID: 36969834]. [PubMed Central ID: PMC10036401]. https://doi.org/10.3389/fphar.2023.1147823.
44. Chen F, Zhang K, Wang M, He Z, Yu B, Wang X, et al. VEGF-FGF Signaling Activates Quiescent CD63(+) Liver Stem Cells to Proliferate and Differentiate. *Adv Sci*. 2024;**11**(33). e2308711. [PubMed ID: 38881531]. [PubMed Central ID: PMC11434209]. https://doi.org/10.1002/advs.202308711.
45. Wu Z, Shangguan D, Huang Q, Wang YK. Drug metabolism and transport mediated the hepatotoxicity of Pleuropterus multiflorus root: a review. *Drug Metab Rev*. 2024;**56**(4):349-58. [PubMed ID: 39350738]. https://doi.org/10.1080/03602532.2024.2405163.
46. Baykalir BG, Arslan AS, Mutlu SI, Parlak Ak T, Seven I, Seven PT, et al. The protective effect of chrysin against carbon tetrachloride-induced kidney and liver tissue damage in rats. *Int J Vitam Nutr Res*. 2021;**91**(5-6):427-38. [PubMed ID: 32349632]. https://doi.org/10.1024/0300-9831/a000653.
47. Wu Z, Sun W, Wang C. Retrospective analysis of clinical features of liver injury induced by levofloxacin. *Expert Opin Drug Saf*. 2025:1-7. [PubMed ID: 40232390]. https://doi.org/10.1080/14740338.2025.2494685.
48. Smith AK, Ropella GEP, McGill MR, Krishnan P, Dutta L, Kennedy RC, et al. Contrasting model mechanisms of alanine aminotransferase (ALT) release from damaged and necrotic hepatocytes as an example of general biomarker mechanisms. *PLoS Comput Biol*. 2020;**16**(6). e1007622. [PubMed ID: 32484845]. [PubMed Central ID: PMC7292418]. https://doi.org/10.1371/journal.pcbi.1007622.
49. He J, Feng X, Liu Y, Wang Y, Ge C, Liu S, et al. Graveoline attenuates D-GalN/LPS-induced acute liver injury via inhibition of JAK1/STAT3 signaling pathway. *Biomed Pharmacother*. 2024;**177**:117163. [PubMed ID: 39018876]. https://doi.org/10.1016/j.biopha.2024.117163.
50. Qiao H, Ren H, Liu Q, Jiang Y, Wang Q, Zhang H, et al. Anti-inflammatory effects of Rehmannia glutinosa polysaccharide on LPS-induced acute liver injury in mice and related underlying mechanisms. *J Ethnopharmacol*. 2025;**351**:120099. [PubMed ID: 40484254]. https://doi.org/10.1016/j.jep.2025.120099.
51. Chou AH, Lee HC, Liao CC, Yu HP, Liu FC. ERK/NF-kB/COX-2 Signaling Pathway Plays a Key Role in Curcumin Protection against Acetaminophen-Induced Liver Injury. *Life*. 2023;**13**(11). [PubMed ID: 38004290]. [PubMed Central ID: PMC10672507]. https://doi.org/10.3390/life13112150.
52. Heo YJ, Lee N, Choi SE, Jeon JY, Han SJ, Kim DJ, et al. Amphiregulin Induces iNOS and COX-2 Expression through NF-kappaB and MAPK Signaling in Hepatic Inflammation. *Mediators Inflamm*. 2023;**2023**:2364121. [PubMed ID: 37868614]. [PubMed Central ID: PMC10586434]. https://doi.org/10.1155/2023/2364121.
53. Niu WH, Wu F, Cao WY, Wu ZG, Chao YC, Liang C. Network pharmacology for the identification of phytochemicals in traditional Chinese medicine for COVID-19 that may regulate interleukin-6. *Biosci Rep*. 2021;**41**(1). [PubMed ID: 33146673]. [PubMed Central ID: PMC7809559]. https://doi.org/10.1042/BSR20202583.
54. Li N, Sun W, Zhou X, Gong H, Chen Y, Chen D, et al. Dihydroartemisinin Protects against Dextran Sulfate Sodium-Induced Colitis in Mice through Inhibiting the PI3K/AKT and NF-kappaB Signaling Pathways. *Biomed Res Int*. 2019;**2019**:1415809. [PubMed ID: 31781591]. [PubMed Central ID: PMC6875009]. https://doi.org/10.1155/2019/1415809.
55. Fergusson AD, Zhang R, Riffle JS, Davis RM. Encapsulation of PI3K Inhibitor LY294002 within Polymer Nanoparticles Using Ion Pairing Flash Nanoprecipitation. *Pharmaceutics*. 2023;**15**(4). [PubMed ID: 37111642]. [PubMed Central ID: PMC10145332]. https://doi.org/10.3390/pharmaceutics15041157.
56. Pu X, Fu Y, Yang Y, Xu G. Ginkgo biloba extract alleviates CCl(4)-induced acute liver injury by regulating PI3K/AKT signaling pathway. *Heliyon*. 2024;**10**(4). e26093. [PubMed ID: 38390084]. [PubMed Central ID: PMC10881365]. https://doi.org/10.1016/j.heliyon.2024.e26093.